International Journal of Technology

http://ijtech.eng.ui.ac.id

Research Article

Finite Element-Based Evaluation of Fiber Orientation Effects on Sisal and Kenaf Fiber-Reinforced Composites for Lightweight Energy Applications

Julendra Bambang Ariatedja[1], Alief Wikarta[1], I Made Londen Batan[1*], Agus Sigit Pramono[1], Suwarno[1], Putu Suwarta[1], Sze Wei Khoo[2], Ubaidillah[3],

[1]Department of Mechanical Engineering, Institut Teknologi Sepuluh Nopember, 60111, Sukolilo, Surabaya, East Java, Indonesia

[2]Department of Industrial Engineering, Universiti Tunku Abdul Rahman, Jalan Universiti, Bandar Barat, 31900 Kampar, Perak, Malaysia

[3]Department of Mechanical Engineering, Universitas Sebelas Maret Solo, 57126, Surakarta, Central Java, Indonesia

[*]Corresponding author: londbatan@me.its.ac.id; Tel.: +62-878-0300-1654

Abstract: Natural fiber reinforced composites (NFRCs) provide a sustainable substitute for synthetic materials; however, enhancing their mechanical performance is difficult. This study examines the impact of fiber orientation and laminate configuration on the tensile and flexural characteristics of sisal and kenaf fiber-reinforced composites. The results indicate that the yield strength of these composites is substantially influenced by the number of 0° laminates. Reducing their quantity leads to a significant loss in yield strength, regardless of whether they are placed in the outer or inner layers. Conversely, the 45° laminates exhibited no impact, whereas the 90° laminates significantly diminished the yield strength. Kenaf fiber-reinforced composites exhibited enhanced stiffness, augmenting the rigidity of the composite by 120% compared with that of sisal fiber-reinforced composites. The flexural modulus was dependent on the laminate orientation and location, with the lack of 0° laminates on the outer layer resulting in a 10% decrease. The flexural modulus determined in the four-point bending test was uniformly 117% of that measured in the three-point bending test, irrespective of the fiber type. The investigation of flexural strength revealed that sisal composites had superior flexural strength compared with kenaf composites. Configurations such as $[(0°)_{10}]$ and $[(0°)_2/(45°)_2/(90°)_2/(-45°)_2/(0°)_2]$ in sisal fibers demonstrate enhanced flexural strength. The kenaf composite with the $[(0°)_{10}]$ structure attained the highest flexural modulus. The findings highlight the influence of laminate orientation on the mechanical performance of NFRCs. Although synthetic fibers still outperform natural fibers in terms of tensile strength, this study emphasizes the potential of kenaf and sisal fibers for applications requiring customized stiffness and strength. These discoveries enhance the advancement of optimized composite designs for renewable energy systems and lightweight structural applications.

Keywords: Fiber orientation; Flexural strength; NFRCs; Tensile strength; Renewable energy

1. Introduction

The global search for synthetic material alternatives has intensified in response to their growing environmental impacts. Synthetic (primarily petrochemical-based) fibers have been widely adopted for their superior mechanical performance, durability, and cost-effectiveness; however, their ecological footprint is concerning. These materials significantly contribute to climate change through greenhouse gas emissions, persist as non-biodegradable waste, and release microplastics into ecosystems. As major consumers of synthetic fibers, the textile and composite industry accounts for 5%–10% of global greenhouse gas emissions and 20% of water pollution

https://doi.org/10.14716/ijtech.v17i2.8003
Received August 2025; Revised September 2025; Accepted February 2026

(Choudhury, 2014). These challenges underscore the urgency of developing materials aligned with the principles of ecological sustainability and circular economy.

In this context, NFRCs have emerged as viable replacements for synthetic composites. These natural composites contain natural fibers embedded in a polymer matrix and offer advantages such as renewability, biodegradability, low density, and adequate mechanical properties (Jawaid and Khalil, 2011). Natural fibers derived from plants, animals, or minerals (Chandramohan and Marimuthu, 2011) include plant-based varieties such as sisal, kenaf, flax, and jute, which are widely studied for their abundance and affordability. In addition to environmental benefits, natural fibers provide several engineering-relevant advantages, including lower embodied energy during production, competitive stiffness-to-weight and strength-to-weight ratios (Shieddieque et al., 2021; Wambua et al., 2003), enhanced vibration damping capability (Alajmi et al., 2022), inherent corrosion resistance, and improved end-of-life disposal options compared to synthetic fibers (Raj et al., 2023). These characteristics make NFRCs particularly attractive for applications where lightweight design, functional performance, and sustainability must be simultaneously addressed (Supian et al., 2024; Supian et al., 2024).

The sisal and kenaf fibers exemplify the potential of NFRCs. Sisal, sourced from the Agave sisalana plant (Joseph et al., 1999), and kenaf, obtained from Hibiscus cannabinus (Wambua et al., 2003), are notable for their mechanical performance and adaptability. Beyond traditional automotive and construction applications, natural fiber composites are increasingly being explored for lightweight components in renewable energy and rotating machinery applications. In automotive engineering, NFRCs are used for dashboards, door trims, seatbacks, interior panels, and non-load-critical structural elements, where weight reduction and vibration damping are critical (Sreenivas et al., 2020; Cheung et al., 2009). Similarly, fan and blade structures, including auxiliary blades and secondary components, benefit from the high specific stiffness and damping characteristics of natural fiber composites (Venkatesan and Bhaskar, 2020).

The role of composite materials in renewable energy systems, such as wind energy conversion, extends beyond strength alone. To ensure aerodynamic efficiency, structural integrity, and long service life, wind turbine blades and fan blades require a careful balance between stiffness tailoring, fatigue resistance, and weight reduction. Optimization of the laminate design for wind turbine structural elements underscores the need for orientation and stacking sequence control for stiffness and weight efficiency (Polit et al., 2021). For instance, flax fiber-reinforced composites can reduce the weight of wind turbine blades, thereby improving energy efficiency (Chinta, Ravinder Reddy, and Prasad, 2022; Chinta, Ravinder Reddy, and Eshwar Prasad, 2022; Miliket et al., 2022; Kalagi et al., 2018; Sundar et al., 2017).

Despite these advantages, NFRC adoption faces challenges. The hydrophilic nature of natural fibers leads to moisture absorption, causing swelling and mechanical degradation over time. Enhancing fiber-matrix bonding, minimizing water uptake, and improving long-term durability require chemical treatments such as alkali (NaOH) or silane coupling agents (Jaiswal et al., 2022; Islam et al., 2022; P. V. Reddy et al., 2021; B. M. Reddy et al., 2020; Giannitra et al., 2019; Pickering et al., 2016; Santhanam and Chandrasekaran, 2014; Malkapuram et al., 2009). Variability in fiber properties due to plant species, growth conditions, and processing methods complicate consistency. Critical parameters, such as fiber volume fraction, orientation, and stacking sequence, directly influence macro-mechanical performance, underscoring the importance of laminate design in achieving performance targets (Moraras et al., 2023; Aravinth et al., 2023; Kennedy and Inigo Raja M, 2022; Chinta, Ravinder Reddy, and Prasad, 2022; Bharath et al., 2022; Gupta et al., 2021; Wang et al., 2019; Al-Ansari, 2014).

Recent research has focused on optimizing these parameters to enhance the properties of NFRC. Studies have demonstrated that tensile and flexural strengths correlate strongly with fiber volume fraction, with higher fractions yielding improved performance (Aravinth et al., 2023; Al-Ansari, 2014; Rao et al., 2010). Fiber orientation is equally critical; for example, $0°/90°$ orientations in kenaf composites enhance tensile strength compared to $\pm 45°$ angles due to efficient stress transfer (Sivakumar et al., 2018). Hybridization—combining natural fibers

with synthetic or other natural fibers—has also been proven effective. For instance, glass/kenaf hybrids exhibit up to 35% higher flexural strength than pure kenaf composites (Zakaria et al., 2023; Yusuff et al., 2021; Selvan et al., 2020; Sharba et al., 2016).

However, clear research gaps remain in the current literature. Most existing studies focus on a single natural fiber type or a limited number of laminate configurations, making generalizing design insights difficult. Direct comparative investigations between different natural fibers—such as sisal and kenaf—conducted under identical modeling and testing frameworks are still scarce.

Furthermore, although computational methods, such as the finite element method (FEM), have modeled composite behavior (Chinta, Ravinder Reddy, and Prasad, 2022; Gupta et al., 2021; Buragohain, 2017), systematic isolation of the individual roles of 0°, ś45°, and 90° plies within multilayer laminates remains limited. Numerical analyses of fiber-reinforced honeycomb composites demonstrate that unidirectional fiber orientation significantly enhances stiffness and load absorption, reinforcing the importance of orientation-based performance tuning (Ariyanti et al., 2022). Comparative evaluations of three- and four-point bending responses in natural fiber-reinforced composites, particularly in the context of lightweight energy-supporting structures, are rarely addressed. This hinders the development of data-driven industrial implementation design frameworks.

1.1 Research Gap and Novelty

To address these gaps, this study provides a systematic finite element-based investigation of sisal and kenaf fiber-reinforced epoxy composites under identical modeling conditions. Leveraging advanced FEM simulations (Moraras et al., 2023; Aravinth et al., 2023), this study aims to optimize design parameters for performance-driven applications, enabling a comparative assessment of both fibers. Unlike most prior studies that examined a single fiber system or a specific layup, this study offers a direct comparison between sisal and kenaf fibers using the same material framework, fiber volume fraction, and laminate thickness. Furthermore, the study explicitly isolates the mechanical contributions of 0°, ±45°, and 90° plies are explicitly isolated by analyzing multiple stacking sequences with controlled orientation variations. In addition, the three- and four-point bending responses were evaluated to elucidate the differences in the stiffness-dominated flexural behavior relevant to lightweight energy-supporting structures. This study advances the understanding of orientation-driven mechanical tailoring in natural fiber composites and provides practical insights for their application in lightweight and renewable energy-related structural components.

1.2 Materials

This study employs natural fibers—sisal and kenaf—as reinforcement materials, combined with an epoxy resin matrix, to fabricate sisal/epoxy and kenaf/epoxy composite laminates with a fiber volume fraction of 40%. The selection of this fiber fraction is informed by previous studies and optimized for both mechanical strength and the strength-to-weight ratio. All specimens were prepared using the unidirectional lamination method. Ten specimens were fabricated with varying fiber orientation configurations, specifically at 0°, ±45°, and 90°, to investigate the effect of anisotropy on mechanical performance. The scheme and the global coordinate system for fiber orientation reference are shown in Supplementary Figures S1, S2, and S3. Table 1 summarizes the material properties of sisal, kenaf, and epoxy resin used in the modeling.

1.3 Orthotropic stress limit

The maximum stress that an orthotropic material—one exhibiting direction-dependent mechanical properties—can sustain prior to failure is defined as the orthotropic stress limit. Composite materials are a typical example of orthotropic materials, characterized by different mechanical responses along different material axes. These limits are generally categorized into two primary orientations: longitudinal and transverse. Longitudinal properties describe the response

of the material along the fiber or principal axis, while transverse properties refer to the behavior perpendicular to this direction. According to Buragohain, 2017, the orthotropic strength limits were calculated using classical micromechanics-based formulations, as summarized in Equations (1) - (6).

Table 1 Mechanical properties of sisal fiber, kenaf fiber, and epoxy matrix used as input parameters in the finite element simulations

Properties	Sisal	Kenaf	Epoxy (Rapid Resin)
Density (g/cm^3)	1.45	1.5	1.16
Young's Modulus (GPa)	7	17.67	3.4
Poisson Ratio	0.44	0.324	0.36
Tensile Strength (MPa)	889.58	450	80

1.3.1 Longitudinal tensile strength

If the longitudinal strain of the matrix is greater than the longitudinal strain of fiber ($\varepsilon_m > \varepsilon_f$), the longitudinal tensile strength equation is as follows:

$$(\sigma_{1c}^T)_{ult} = (\sigma_{1f}^T)_{ult} V_f + (\varepsilon_{1f}^T)_{ult} E_m (1 - V_f)$$

$$(\varepsilon_{1f}^T)_{ult} = \frac{(\sigma_{1f}^T)_{ult}}{E_f} \tag{1}$$

Where $(\sigma_{1c}^T)_{ult}$ is ultimate longitudinal tensile stress of composite, $(\sigma_{1f}^T)_{ult}$ is ultimate longitudinal tensile stress of fiber, $(\varepsilon_{1f}^T)_{ult}$ is ultimate longitudinal tensile strain of fiber, V_f is fiber volume fraction, E_m is elastic modulus of the matrix, and E_f is elastic modulus of the fiber.

If the longitudinal strain of the matrix is less than the longitudinal strain of fiber ($\varepsilon_m < \varepsilon_f$), the longitudinal tensile strength equation is as follows:

$$(\sigma_{1c}^T)_{ult} = (\varepsilon_{1m}^T)_{ult} E_f V_f + (\sigma_{1m}^T)_{ult} (1 - V_f)$$

$$(\varepsilon_{1m}^T)_{ult} = \frac{(\sigma_{1m}^T)_{ult}}{E_m} \tag{2}$$

Where $(\varepsilon_{1m}^T)_{ult}$ is ultimate longitudinal tensile strain of matrix, E_{1f} is Young's modulus in the longitudinal direction of the fiber, and $(\sigma_{1m}^T)_{ult}$ is ultimate longitudinal tensile stress of the matrix.

1.3.2 Longitudinal compressive strength

$$(\sigma_{1c}^C)_{ult} = 2(\tau_{12f})_{ult} \left(V_f + \frac{E_m}{E_f}(1 - V_f) \right)$$

$$(\tau_{12f})_{ult} = \frac{1}{2} \sigma_{1m}^C \frac{E_{1f}}{E_m} \tag{3}$$

Where $(\sigma_{1c}^C)_{ult}$ is ultimate longitudinal compressive strength of composite, $(\tau_{12f})_{ult}$ is ultimate longitudinal shear strength of the fiber, and σ_{1m}^C is longitudinal compressive strength of the matrix.

1.3.3 Transverse tensile strength

$$(\sigma_{2c}^{T})_{ult} = (\sigma_{m}^{T})_{ult}\left(1 - 2\sqrt{\frac{V_f}{r}}\right) \tag{4}$$

Where $(\sigma_{2c}^{T})_{ult}$ is ultimate transverse tensile stress of the composite, and $(\sigma_{m}^{T})_{ult}$ are ultimate tensile strength of the matrix.

1.3.4 Transverse compressive strength

$$(\sigma_{2c}^{C})_{ult} = (\sigma_{m}^{C})_{ult}\left(1 - 2\sqrt{\frac{V_f}{r}}\right) \tag{5}$$

Where $(\sigma_{2c}^{C})_{ult}$ is ultimate transverse compressive stress of the composite, and $(\sigma_{m}^{C})_{ult}$ is ultimate compressive strength of the matrix.

1.3.5 In-plane shear strength

$$(\tau_{12c})_{ult} = G_{12c}\left[1 + \left(\frac{G_m}{G_{12f}} - 1\right)V_f\right](\gamma_m)_{ult}$$

$$G_{12c} = \frac{G_{12f}G_m}{G_m V_f + G_{12f}(1 - V_f)}$$

$$(\gamma_m)_{ult} = \frac{(\tau_m)_{ult}}{G_m} \tag{6}$$

Where $(\tau_{12c})_{ult}$ is ultimate longitudinal shear strength / in-plane shear strength of composite, G_{12c} is shear modulus of the composite in the longitudinal direction, G_m is shear modulus of matrix, G_{12f} is shear modulus of the fiber in the longitudinal direction, $(\gamma_m)_{ult}$ is ultimate shear strain of the matrix, and $(\tau_m)_{ult}$ is ultimate shear strength of the matrix.

The orthotropic stress limit is input into the Engineering Data module in ACP (Pre) following the calculation. This value represents the maximum stress the material can withstand before failure, enabling the prediction of the critical load at which structural failure is most likely to occur.

1.4 Characterization

1.4.1 Tensile Test

The tensile properties of the fabricated composite specimens, namely, the ultimate tensile strength and Young's modulus, were evaluated in accordance with the ASTM D3039 standard. The test specimens were 250 mm in length and 15 mm in width, as illustrated in Supplementary Figure S4. Each specimen was composed of 10 laminae, each with a thickness of 0.3 mm.

1.4.2 Flexural Test

1.4.3 Three-point Bending

The flexural properties of the composite materials were evaluated through three-point bending tests, which were conducted in accordance with the ASTM D790 standard. For the sisal/epoxy composites, specimens with dimensions of 80 mm × 13 mm × 3 mm were prepared, as illustrated in Supplementary Figure S5a. These consisted of 10 laminae, each with a thickness of 0.3 mm. In the case of the kenaf/epoxy composites, the specimen dimensions were 150 mm ×

25.4 mm × 6 mm (Supplementary Figure S5b), comprising 10 laminae each with a thickness of 0.6 mm. The numerical modeling incorporated both the pressing roller and the supports, each modeled as cylindrical components with a diameter of 6 mm. Supplementary Figure S6a shows the boundary conditions for the three-point bending test simulation.

1.4.4 Four-point Bending

In addition to the three-point bending tests, four-point bending tests were conducted to evaluate the composites' pure flexural properties, minimizing the influence of shear stress. Experiments were performed in accordance with the ASTM D6272 standard. The specimen dimensions used for both sisal/epoxy and kenaf/epoxy composites were identical to those employed in the three-point bending tests, i.e., 80 mm × 13 mm × 3 mm for sisal/epoxy and 150 mm × 25.4 mm × 6 mm for kenaf/epoxy. Supplementary Figure 6b illustrates the boundary conditions applied during the four-point bending tests.

The laminae thickness and fiber volume fraction were kept constant for all stacking configurations, ensuring that observed differences arise solely from fiber orientation and stacking sequence.

2. Simulation Procedure

The composite material behavior was simulated using a multistep approach that aligns with experimental testing standards and ensures the physical representativeness of the numerical model. The procedure comprised the following key stages:

Material Definition: The mechanical properties of the constituent materials—sisal fibers, kenaf fibers, and epoxy resin—were defined, including Young's modulus, Poisson's ratio, and tensile strength. These data were input into the Engineering Data module. Subsequently, the Material Designer was utilized to generate the effective homogenized properties of the composite laminate by specifying the fiber and matrix types, volume fractions (40% fiber), and composite type (unidirectional laminate). The Material Designer output includes orthotropic material properties, which were then used in the analysis.

Geometry and Meshing: The geometry of the specimens was modeled according to ASTM D3039 for tensile tests and ASTM D790/D6272 for three- and four-point bending tests. Meshing was performed using hexahedral or tetrahedral elements with mesh refinement focused on the central region (gauge length for tensile, span for bending) to accurately capture stress and deformation gradients.

Layup Definition: Using the ACP (Pre) module, the laminate structure was defined by specifying the stacking sequence, fiber orientation angles (0°, ±45°, and 90°), and the thickness of each lamina (0.3 mm for sisal, 0.6 mm for kenaf). To assess the influence of fiber orientation, multiple layup configurations were modeled.

Boundary Conditions: Boundary conditions were defined in Static Structural to precisely replicate the mechanical testing environment:

Tensile Test:

- One end of the specimen (typically the left face) was fixed in all degrees of freedom (displacement and rotation).
- A uniaxial tensile load or displacement was applied to the opposite end (right face) in the axial (longitudinal) direction.
- Lateral constraints were released to allow Poisson's effect, mimicking realistic deformation.

Three-Point Bending Test:

- Two cylindrical supports were modeled under the specimen at specified spans (ASTM-compliant).

- A single cylindrical roller applied the load from above at the center of the span.
- The supports were modeled as frictionless contacts with S2 interaction.
- Constraints: The bottom supports restricted vertical displacement (Y-direction) and rotation, whereas the loading roller allows vertical motion and applies a prescribed displacement or force.

Four-Point Bending Test:

- Similar to three-point bending but with two loading rollers placed symmetrically between the supports to create a constant moment region in the middle of the span.
- The setup eliminates mid-span shear effects, allowing pure bending analysis.
- To prevent unrealistic stress concentration, all contact interfaces (supports and loading noses) were modeled using surface-to-surface frictionless contacts.

Supplementary Figures S7 and S8 illustrate the simulation workflow and meshed models used for tensile and flexural analysis, respectively. The simulation was executed to evaluate key mechanical response parameters such as normal stress distribution, elastic strain, and directional deformation upon completion of the setup. These results were then analyzed to assess the influence of laminate configurations on the composite materials' mechanical performance.

The present study focuses exclusively on the evaluation of tensile and flexural behavior through finite element simulations based on ASTM D3039, ASTM D790, and ASTM D6272 standards. Impact testing and associated damage evolution analyses were not included in this study. Consequently, we did not consider experimental configurations such as impact or drop-weight testing. This limitation is intentional because the primary objective of the study is to investigate the influence of laminate orientation and stacking sequence on stiffness- and strength-dominated responses under quasi-static loading conditions.

3. Results and Discussion

3.1 Tensile Properties

Table 2 shows the tensile test results for the sisal/epoxy and kenaf/epoxy composites, which highlight the significant influence of fiber orientation on both tensile strength and elastic deformation. The unidirectional $[(0°)_{10}]$ configuration, where all fibers are aligned with the loading axis, demonstrated the highest tensile strength. This configuration allows optimal load transfer along the fiber direction, maximizing the fibers' reinforcing effect and resulting in a tensile-resistant composite.

Table 2 Tensile and flexural test results

Mark	Configuration	Tensile				3 Point Bending				4 Point Bending			
		Tensile strength (MPa)		Elastic modulus (GPa)		Flexural strength (MPa)		Flexural modulus (GPa)		Flexural strength (MPa)		Flexural modulus (GPa)	
		Sisal	Kenaf	Sisal	Kenaf	Sisal	Kenaf	Sisal	Kenaf	Sisal	Kenaf	Sisal	Kenaf
010	$[0°]_{10}$	179.15	81.14	4.67	6.18	247.69	171.80	5.45	5.68	167.80	132.14	6.30	6.67
08A	$[0°]_4/(45°)_2/(0°)_4$	173.65	81.01	4.67	6.17	247.80	171.90	5.45	5.67	167.91	132.25	6.30	6.65
08B	$[0°]_4/(90°)_2/(0°)_4$	70.47	42.50	4.67	6.17	247.85	171.94	5.44	5.67	167.95	132.28	6.30	6.66
04	$[0°]_2/(45°)_2/(90°)_2/(-45°)_2/(0°)_2$	70.64	43.19	4.67	6.17	250.00	175.05	5.36	5.56	170.90	134.97	6.16	6.50
-4A	$[(45°)_2/(0°)_2/(45°)_2/(0°)_2/(45°)_2]$	48.04	21.07	4.31	5.23	244.62	168.70	5.13	5.25	165.27	129.46	5.93	6.07
-4B	$[(-45°)_2/(0°)_2/(45°)_2/(0°)_2/(-45°)_2]$	47.58	20.56	4.28	5.16	244.62	168.71	5.13	5.25	165.27	129.45	5.93	6.06
-4C	$[(90°)_2/(0°)_2/(90°)_2/(0°)_2/(90°)_2]$	27.93	13.62	4.22	5.09	242.43	166.76	5.09	5.21	164.30	128.59	5.86	5.99
-2	$[(45°)_2/(-45°)_2/(0°)_2/(-45°)_2/(45°)_2]$	48.99	21.92	4.34	5.31	247.66	171.89	5.06	5.15	167.59	132.13	5.84	5.92
-0A	$[(45°)_{10}]$	49.03	21.23	4.34	5.31	247.81	171.96	5.04	5.14	167.72	132.32	5.83	5.90
-0B	$[(-45°)_2/(45°)_2/(-45°)_2/(45°)_2/(-45°)_2]$	48.72	21.65	4.34	5.30	247.78	172.00	5.05	5.14	167.70	132.24	5.84	5.91

Footnote: The green highlighted values indicate the highest performance in each test category and vice versa for those values inside the double-line box.

The hybrid configuration $[(0°)_4/(45°)_2/(0°)_4]$ also exhibited favorable tensile performance, although slightly lower than the fully aligned $[(0°)_{10}]$ arrangement. This indicates that introducing ±45° fibers can provide additional in-plane toughness, albeit with a modest reduction

in the axial tensile strength. In terms of stiffness, the [(0°)10] configuration again yielded the highest elastic modulus, reflecting its superior ability to resist elastic deformation along the load direction. The modulus values observed for the $[(0°)_4/(45°)_2/(0ř°)_4]$ configuration were notably high, indicating that the partial alignment of fibers with the loading axis continues to significantly contribute to stiffness.

Sisal-reinforced composites exhibited higher tensile strength than their kenaf counterparts across all lamination configurations, although both materials showed comparable values in terms of elastic modulus. This indicates that while sisal fibers exhibit superior resistance to failure under axial load, kenaf fibers demonstrate a comparable elastic response. Thus, the choice of fiber orientation should be tailored to specific mechanical requirements. A 0° fiber orientation is most effective for axial load-bearing applications, while a 90° orientation—perpendicular to the load direction—offers minimal resistance to tensile loads and is generally not recommended when tensile strength is a primary design criterion.

Figures 1 and 2 illustrate the relationship between fiber orientation and mechanical performance metrics, such as yield strength and flexural modulus. Some of these figures include grouped data to highlight comparative trends, while inset plots in the corner provide additional information on elastic modulus or flexural strength, offering a more comprehensive interpretation of orientation-dependent behavior.

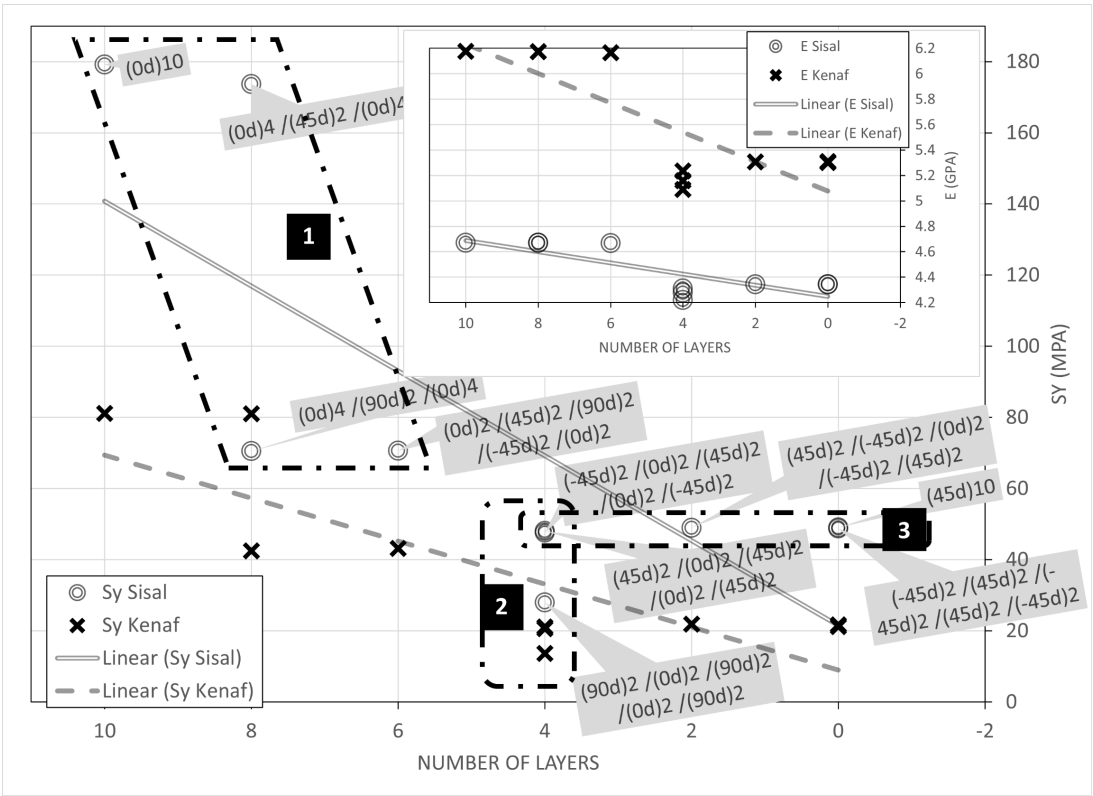

Figure 1 Yield strength versus number of layers at 0°. Inset image: Elastic modulus versus 0° number of layers

3.1.1 Effect of Fiber Orientation on Yield Strength

The results presented in Figure 1 demonstrate that a reduction in the number of 0° laminates significantly decreases the yield strength. Within the first specimen group, composites that preserved 0° laminates on the outer layers exhibited markedly different behaviors depending on the type of inserted intermediate laminae. Specifically, the inclusion of 90° laminates caused a drastic reduction in yield strength—up to an order of magnitude—compared with the configurations incorporating ±45° laminates.

For example, the lamination sequence $[(0°)_2/(45°)_2/(90°)_2/(-45°)_2/(0°)_2]$ yielded a tensile performance comparable to that of $[(0°)_4/(90°)_2(0°)_4]$. The results indicate that replacing certain 0° laminates with 45° or -45° laminates does not significantly affect the yield strength of the composite. Conversely, replacing them with 90° laminates—aligned perpendicular with the loading axis—substantially undermines the axial load-bearing capacity.

In the second group of specimens—where the outer layers do not consist of 0° laminates—a significant reduction in yield strength was observed. This highlights the critical role of outer-layer alignment, with exterior configurations lacking 0° laminates exhibiting compromised structural performance. Similar to the first group, the inclusion of 90° laminates led to a pronounced decline in yield strength, confirming their detrimental effect due to their orientation being perpendicular to the loading axis.

In the third group, the replacement of 0° laminates with ±45° laminates did not result in a substantial reduction in the yield strength. Although ±45° laminates are not as effective as 0° fibers in bearing axial loads, they can still contribute to load transfer and maintain structural integrity without significantly compromising performance.

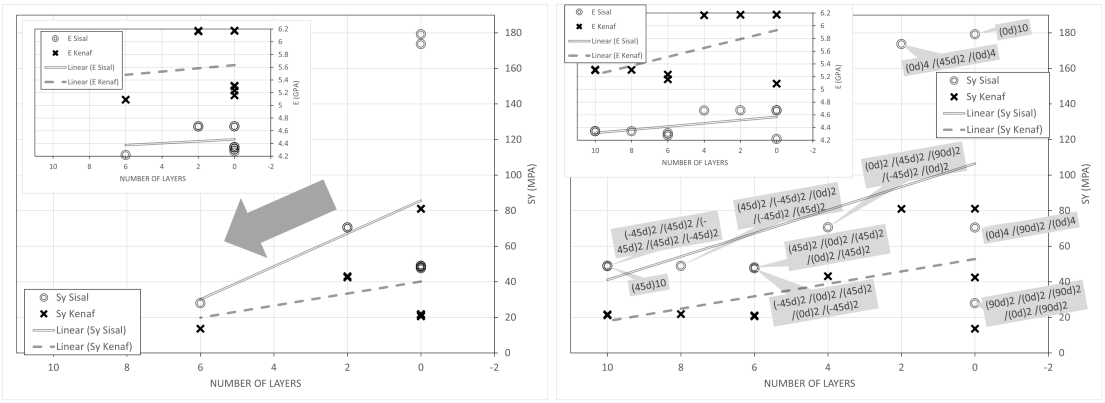

(a) (b)

Figure 2 (a) Yield strength versus number of layers45°. (b) Elastic modulus versus number of layerss 0°

Figure 2a clearly illustrates the inverse relationship between the number of 90° laminates and yield strength—i.e., the greater the proportion of 90° laminates, the lower the yield strength. In contrast, Figure 2b demonstrates that when ±45° laminates dominate the stacking sequence (constituting more than 50% of the total laminae) and 90° laminates are excluded, variations in laminate orientation have a minimal effect on yield strength.

These trends were consistent across both sisal- and kenaf-fiber-reinforced composites. However, kenaf composites exhibited yield strength values approximately 50% lower than those of their sisal counterparts. This underscores the superior axial load-bearing capability of sisal fibers in laminated composites. Collectively, these findings offer valuable insights for optimizing laminate architecture to enhance yield strength in natural fiber-reinforced composite structures.

3.1.2 Fiber orientation on the elastic modulus

The influence of the fiber orientation configuration on the elastic modulus exhibits a trend analogous to that observed for the yield strength, albeit with an inverse relationship. Specifically, configurations that reduce yield strength tend to correspond with increased elastic modulus and vice versa. This inverse pattern highlights the inherent trade-off between strength and stiffness in fiber-reinforced composites.

The elastic modulus of kenaf fiber-reinforced composites reached approximately 120% of the value attained by sisal-based composites. This indicates that despite both composite systems demonstrating similar trends in how fiber orientation and laminate composition affect elastic response, kenaf fibers contribute more significantly to enhancing the material's overall stiff-

ness. Therefore, while sisal fibers offer superior tensile strength, kenaf fibers present a distinct advantage in applications where structural rigidity and high elastic modulus are prioritized.

3.2 Flexural Properties

3.2.1 Three-point Bending

As summarized in Table 2, flexural testing of the composites revealed that variations in fiber orientation angle significantly influenced both the flexural strength and stiffness of the materials. Although the configurations differed relatively moderately, certain fiber angle combinations yielded superior performance. The highest flexural strength was achieved with the $[(0°)_2/(45°)_2/(90°)_2/(-45ř°)_2/(0°)_2]$ configuration. For this layup, the sisal/epoxy composite reached a peak flexural stress of 250.9 MPa, while the kenaf/epoxy counterpart attained 175.05 MPa. Conversely, the poorest performance was recorded for the $[(90°)_2/(0°)_2/(90°)_2/(0°)_2(90°)_2]$ configuration, highlighting the detrimental impact of placing 90° laminates at the outer layers in flexural loading conditions. Further, flexural modulus calculations revealed that the $[(0°)_{10}]$ configuration exhibited the highest stiffness, with values of 5.448 GPa for sisal/epoxy and 5.675 GPa for kenaf/epoxy composites. In contrast, the $[(45°)_{10}]$ layup resulted in the lowest flexural modulus, measured at 5.040 GPa for sisal/epoxy and 5.141 GPa for kenaf/epoxy, respectively.

3.2.2 Four-point Bending

The results of the four-point bending tests demonstrated that the fiber orientation significantly influenced the composites' flexural performance. The highest flexural strength was observed in the $[(0°)_2/(45°)_2/(90°)_2/(-45°)_2/(0°)_2]$ configuration, with the sisal/epoxy composites reaching a peak flexural stress of 170.9 MPa and the kenaf/epoxy composites reaching 134.7 MPa. In contrast, the lowest flexural strength was recorded for the $[(90°)_2/(0°)_2/(90°)_2/(0°)_2(90°)_2]$ configuration, with flexural stress values of 164.3 and 128.59 MPa for sisal/epoxy and 128.59 MPa for kenaf/epoxy, respectively. Although the variation between maximum and minimum values is relatively small, the data confirm that the presence and positioning of 90° laminates consistently reduce flexural performance.

Regarding stiffness, the calculated flexural modulus values showed that the unidirectional $[(0°)_10]$ layup resulted in the highest modulus—6.302 GPa for sisal/epoxy and 6.669 GPa for kenaf/epoxy—indicating superior resistance to flexural deformation. Conversely, the $[(45°)_10]$ configuration yielded the lowest flexural modulus values, measured at 5.833 GPa for sisal/epoxy and 5.902 GPa for kenaf/epoxy. The results indicate that fiber alignment in the direction of the load substantially increases flexural rigidity, while orientations such as ±45° contribute less to bending stiffness.

3.2.3 Fiber orientation on the flexural modulus

Figures 3 and 4 show the relationship between the number of layers in specific fiber orientations and the flexural modulus of the laminated composites. Several figures include group classifications to distinguish configuration trends, while inset plots in the corners of each figure provide complementary data on flexural strength.

Figure 3 shows a consistent decrease in flexural modulus as the number of 0° laminates decreases. In the first group—composites with 0° laminates retained on the outer layers—the inclusion of 45° or 90° laminates in the midplane did not significantly affect the flexural modulus. However, in the second group, where the outer layers are not 0° laminates, the flexural modulus is reduced by approximately 10%, suggesting that the outer layer orientation plays a secondary but notable role. Nevertheless, across both groups, laminate orientation appears to have a more limited effect on flexural stiffness than on tensile or yield strength.

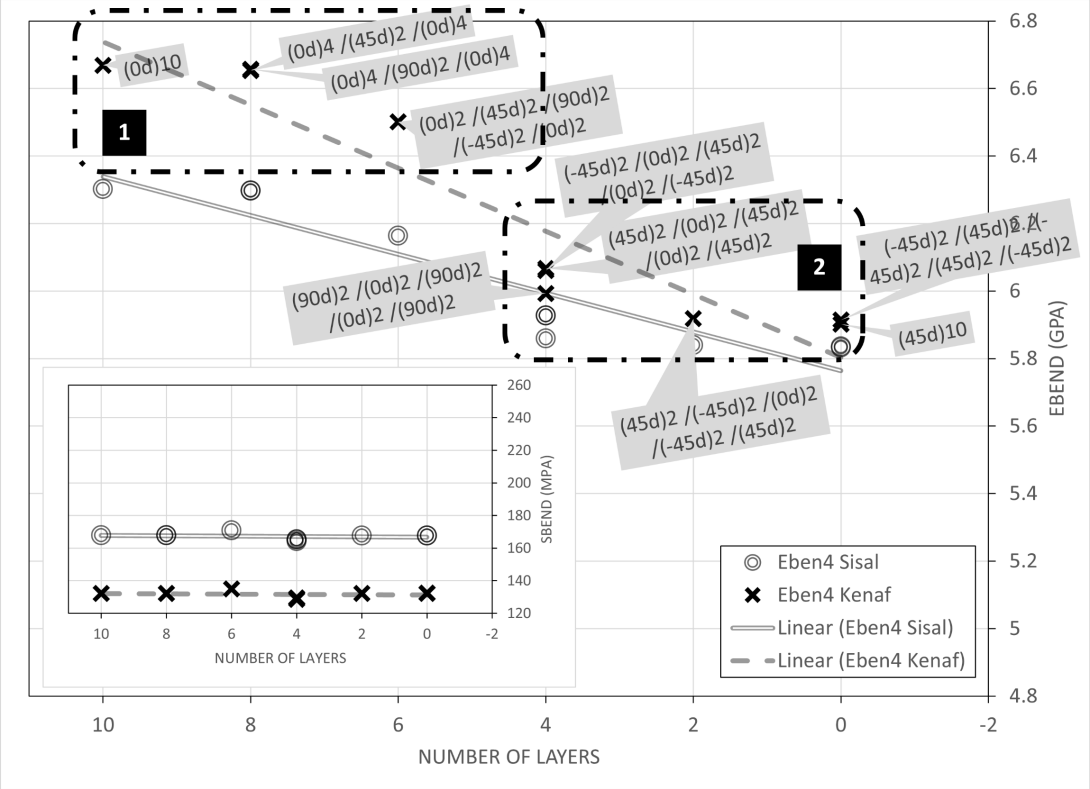

Figure 3 Four-point-bending flexural modulus versus number of 0° layers. Inset image: Four-point-bending flexural strength versus 0° number of layers

Figure 4b further supports this observation, showing that the number of 45° laminates does not substantially alter the flexural modulus. A comparison between Figures 4a and 4b reveals that the flexural modulus obtained from the four-point bending tests is approximately 117% of that measured in the three-point bending tests, indicating a reduced shear influence in the four-point configuration.

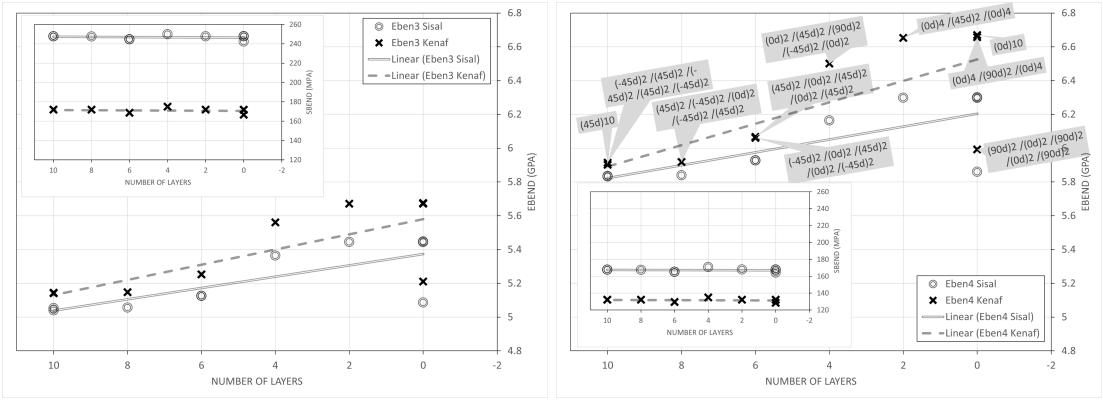

(a) (b)

Figure 4 Flexural modulus of (a) three- and (b) four-point bending versus 45° number of layers. Inset image: Bending strength of (a) three- and (b) four-point bending versus 45° number of layers

These trends were consistently observed for both sisal and kenaf fiber-reinforced composites. Notably, the flexural modulus values of the kenaf-based composites were up to 120% higher than those of the sisal-based composites, reaffirming the superior stiffness characteristics of kenaf. These findings provide meaningful insights into laminate design strategies, particularly for optimizing flexural stiffness in natural fiber-reinforced composites under various bending

conditions. Effect of Fiber Orientation on Flexural Strength.

The insets in Figures 3 and 4 demonstrate that fiber orientation has a limited effect on flexural strength. This indicates that flexural strength is less sensitive to variations in laminate stacking sequences than flexural modulus or tensile strength. Moreover, the results of the three-point bending tests revealed significantly higher flexural strength values than those obtained from the four-point bending tests. Specifically, sisal fiber-reinforced composites exhibit an increase of approximately 50%, while kenaf fiber-reinforced composites show an increase of approximately 25%, as depicted in the insets in Figures 3 and 4a.

Furthermore, a comparative analysis between the two fiber types shows that the flexural strength of kenaf-based composites ranges from approximately 70% (in three-point bending) to 80% (in four-point bending) of that achieved by sisal-based composites. These findings highlight the superior flexural performance of sisal fibers and the influence of the testing method on the reported strength values. Taken together, the results provide valuable insights for selecting appropriate testing methods and fiber types when optimizing the flexural strength of natural fiber-reinforced composites. The choice between three- and four-point bending configurations should consider both the role of shear effects and the specific mechanical property being targeted in the design process.

3.3 Further Comparison

A comparative analysis was conducted to evaluate the mechanical properties of the fabricated natural fiber composites against a range of other natural and synthetic composite materials. This comparison provides a broader perspective on the performance positioning of sisal and kenaf fiber-reinforced composites within the composite engineering materials landscape.

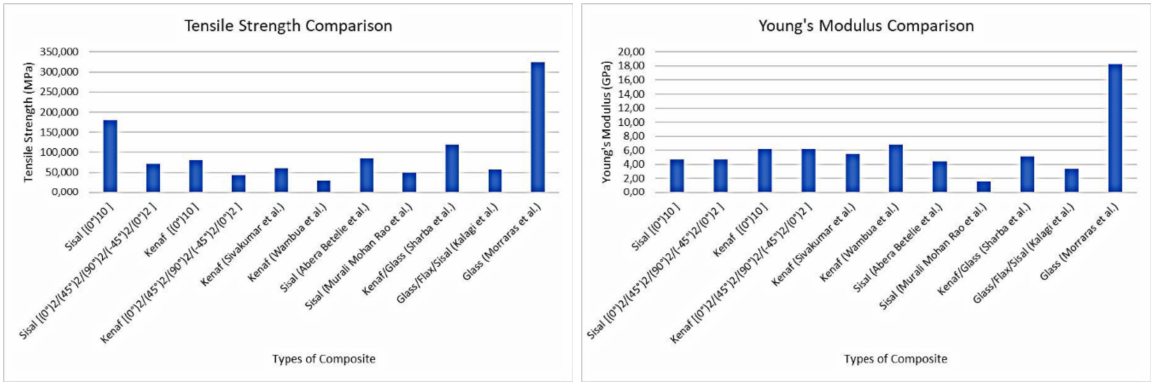

(a) (b)

Figure 5 (a) Comparison of tensile strength and (b) Young's modulus among various composite materials

Tensile Properties: As illustrated in Figure 5a, the sisal/epoxy composite with the $[(0°)_{10}]$ layup exhibited the highest tensile strength among the natural fiber composites examined. Remarkably, this configuration outperformed even hybrid composites such as the kenaf/glass system studied by Sharba et al., 2016, which employed a 3G/K/3G laminate stacking and a thickness of 5.85 mm. The tensile strength of this hybrid was lower than that of the optimized sisal laminate despite the integration of synthetic glass fiber. However, as expected, fully synthetic fiber composites still dominate in terms of tensile performance. The glass/epoxy composite reported by Moraras et al., 2023, with a $[(0/90°)_5]$ configuration and 4 mm thickness, demonstrated the highest overall tensile strength. Although natural fiber composites fall short in terms of absolute strength compared to synthetics, their environmental benefits and competitive mechanical characteristics affirm their potential as sustainable alternatives.

Elastic Modulus (Stiffness): Figure 5b presents the comparative Young's modulus values, providing insight into material stiffness. As anticipated, the glass fiber composites (Moraras et al., 2023) exhibited the highest Young's modulus, reflecting their superior resistance to

elastic deformation. Among natural fiber systems, the kenaf/PP composite (Wambua et al., 2003)—comprising randomly oriented kenaf fibers at 40% fiber weight fraction—ranked second, indicating the significant stiffness potential of kenaf fibers. Sisal-based composites, while generally demonstrating lower modulus values than kenaf, still achieved moderate stiffness, reinforcing their viability in structural applications requiring intermediate rigidity. Overall, both sisal and kenaf remain less stiff than glass, although kenaf demonstrates a relative advantage in modulus over sisal.

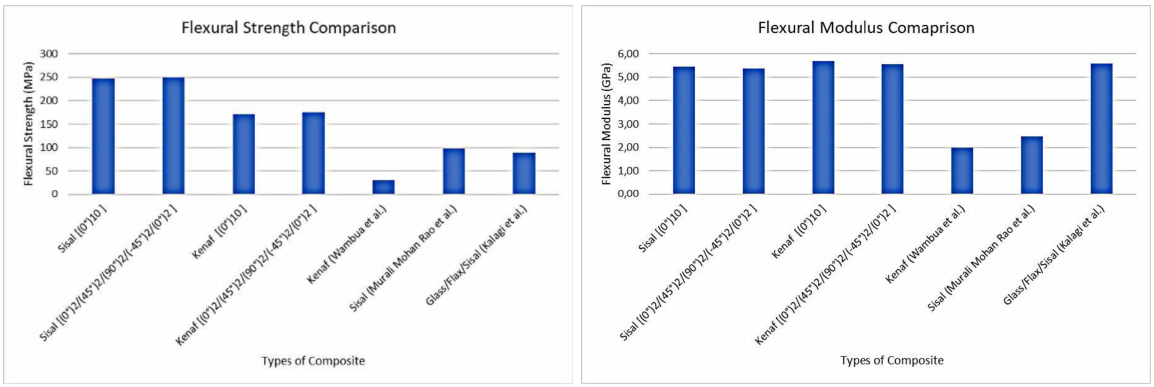

(a) (b)

Figure 6 (a) Comparison of flexural strength and (b) flexural modulus among various composite materials

Flexural Strength: The flexural strength comparisons in Figure 6a further underscore the competitiveness of sisal composites. The sisal $[(0°)_{10}]$ and sisal $[(0°)_2/(45°)_2/(90°)_2/(-45°)_2/(0°)_2]$ configurations achieved among the highest flexural strength values across all composite types. In contrast, the kenaf composites reported by Wambua et al., 2003. displayed the lowest flexural strength, indicating limitations when fiber dispersion is random and not directionally optimized. This confirms the importance of fiber orientation and structural configuration in flexural resistance maximization.

Flexural Modulus: Figure 6b provides a comparative overview of flexural stiffness. The kenaf $[(0°)_{10}]$ configuration exhibited the highest flexural modulus, followed closely by the multidirectional kenaf laminate $[(0°)_2/(45°)_2/(90°)_2/(-45°)_2/(0°)_2]$, and the hybrid glass/flax/sisal-epoxy composite described by Kalagi et al., 2018, with a balanced sequence of $[(0°/90°)_S/(-45°/45°)_F/(0°/90°)_G/(-45°/45°)_F/(0°/90°)_S]$. The sisal composites also showed strong flexural modulus performance, particularly with the $[(0°)_2/(45°)_2/(90°)_2/(-45°)_2/(0°)_2]$ configuration, which slightly trailed the $[(0°)_{10}]$ laminate. At the lower end of the spectrum, kenaf composites (Wambua et al., 2003) and unidirectional sisal composites (Rao et al., 2010) with a fiber volume fraction of 0.39 and a thickness of 3 mm exhibited flexural modulus values of 2.0 GPa and 2.46 GPa, respectively—substantially lower than those achieved by the optimized multidirectional laminates.

Comparison of Natural and Synthetic Fiber Composites. The results confirm that synthetic fiber-reinforced composites outperform natural fiber composites in terms of absolute tensile strength, particularly when glass fibers are used (Venkatesan and Bhaskar, 2020). This performance gap can be primarily attributed to the fundamental material and microstructural differences between natural cellulose-based fibers and synthetic glass fibers (Supian et al., 2024). Compared with cellulose fibers, glass fibers possess a significantly higher intrinsic elastic modulus and tensile strength, enabling more efficient load transfer along the fiber direction under axial loading (Prabaharan et al., 2023).

In addition, natural fibers exhibit greater variability in fiber diameter and cross-sectional geometry, which introduces nonuniform stress distribution within the composite laminate (Palani et al., 2024). Such variability increases the likelihood of localized stress concentrations, which reduces the effective load-bearing capacity. The interfacial bonding between natural fibers and

polymer matrices remains less optimal than that between natural fibers and glass fibers, even with surface treatments, due to the hydrophilic nature of cellulose and the resulting interfacial incompatibility (Karthick et al., 2022). Furthermore, natural fiber composites are more sensitive to defects, such as micro-voids, fiber waviness, and lumen-related imperfections, which can initiate premature failure under tensile loading. Collectively, these factors explain why synthetic fiber composites continue to demonstrate superior tensile performance despite the growing maturity of natural fiber composite technologies (Saroj and Nayak, 2021).

Potential of Sisal and Kenaf Fibers for Customized Stiffness and Strength. Although natural fibers exhibit lower absolute strength than synthetic fibers, the results demonstrate that sisal and kenaf fibers offer significant potential for tailoring mechanical properties through laminate design. Laminate orientation emerges as an effective stiffness- and strength-tuning mechanism, enabling designers to prioritize specific performance requirements without altering the material composition or fiber volume fraction.

Kenaf fiber-reinforced composites consistently exhibited higher elastic and flexural modulus values, indicating their suitability for stiffness-dominated design scenarios, where the primary requirement is deformation resistance. This behavior is associated with the relatively higher longitudinal modulus of kenaf fibers, which enhances laminate rigidity when aligned along the load direction. In contrast, sisal fiber-reinforced composites demonstrated superior tensile and flexural strength, making them more appropriate for strength-dominated applications where resistance to failure under peak loading is critical.

This complementary behavior highlights the strategic role of fiber selection in combination with laminate orientation. Rather than competing directly with synthetic fibers on absolute strength, sisal and kenaf composites enable customized mechanical responses through orientation-driven design, supporting application-specific optimization.

Implications for Optimized Composite Design for Renewable Energy Systems. The findings of this study provide direct implications for the design of composite components supporting renewable energy, particularly those governed by stiffness, weight, and cyclic loading considerations (Owen et al., 2024). In stiffness-driven components such as fan blades, auxiliary wind turbine elements, and lightweight energy-supporting structures, tailoring flexural rigidity through laminate configuration is often more critical than maximizing tensile strength.

In renewable energy systems, weight reduction remains a central design objective because lower structural mass reduces inertial loads, improves energy efficiency, and mitigates fatigue damage under cyclic operation (Samuel et al., 2024). With their low density and orientation-dependent stiffness, natural fiber composites offer a promising balance between mechanical performance and lightweight design requirements (Supian et al., 2024).

The finite element-based approach adopted in this study provides a practical pre-design framework, enabling engineers to screen laminate configurations, evaluate stiffness and strength trade-offs, and optimize stacking sequences prior to experimental validation (Owen et al., 2024; Phunpeng et al., 2023; Cutolo et al., 2021). Such a framework reduces development time and material waste, supporting more efficient composite design workflows for renewable energy applications (Marin-Tellez et al., 2025; Rahman and Sultana, 2023). Recent advances in FEM modeling of natural fiber composites have demonstrated excellent agreement with experimental results, validating the use of computational methods for preliminary design optimization (Naveen et al., 2019).

Deterministic Nature of the FEM and Sensitivity Considerations. Notably, the finite element simulations conducted in this study are deterministic, producing repeatable results under identical input conditions. Consequently, statistical variability, such as standard deviation or error bars commonly associated with experimental testing, is not applicable. Instead, the comparative trends observed across stacking sequences serve as sensitivity indicators, reflecting the influence of fiber orientation and laminate configuration on mechanical response. This deterministic framework allows for controlled isolation of design variables, providing clear insights into changes in orientation-driven performance.

Influence of the Stacking Sequence on the Peak Force Response. The observed differences in peak force among various stacking sequences can be explained by the interaction between the laminate's axial and transverse load-bearing mechanisms (Kumpati et al., 2024; Cakiroglu and Bekdas, 2021). Plies oriented at 0° act as the primary load-bearing layers, resisting axial tensile and bending stresses. Therefore, increasing the proportion of 0° plies enhances the peak force capacity through more efficient stress transfer along the fiber direction (Palani et al., 2024; Cutolo et al., 2021).

The inclusion of 90° plies contributes to transverse stiffness and buckling restraint, thereby limiting lateral deformation and stabilizing the laminate under bending loads (Istana et al., 2024). This transverse constraint improves load redistribution among plies, particularly in hybrid configurations such as [0/90°], resulting in a higher peak force compared to laminates dominated by off-axis orientations (Gebremichael et al., 2025). The interaction between the axial stress carried by 0° plies and the transverse constraint provided by 90° plies leads to a synergistic strengthening effect, explaining the enhanced performance observed in selected stacking sequences (Sinitsky et al., 2022).

3.4 Validation and Future Research

The mechanical trends obtained in this study are consistent with the established understanding of the role of fiber orientation in governing load transfer and stress distribution within composite laminates. Previous studies have shown that plies aligned with the loading direction enhance axial stiffness and delay crack initiation, whereas off-axis plies primarily contribute to transverse constraint and deformation control (Purnowidodo et al., 2018). The present findings extend this understanding to natural fiber-reinforced composites, demonstrating that orientation-driven laminate design can partially offset the lower intrinsic strength of cellulose-based fibers. Similar observations have been reported for natural fiber composites in lightweight automotive applications, where advantages such as low density, corrosion resistance, and inherent vibration damping compensate for reduced absolute strength (Shieddieque et al., 2021). The importance of laminate optimization is further emphasized in renewable energy-related components, including wind turbine and fan blade structures, where stiffness-to-weight efficiency and deformation control are often more critical than peak tensile strength (Polit et al., 2021). Numerical investigations on natural fiber-reinforced sandwich and honeycomb structures have demonstrated that unidirectional and hybrid stacking sequences significantly enhance flexural stiffness and load-bearing efficiency through controlled stress redistribution (Ariyanti et al., 2022). Collectively, these findings support the validity of the finite element-based orientation analysis adopted in this study and confirm its suitability as a pre-design tool for stiffness-dominated, lightweight energy-supporting composite structures.

Although the present study relies on deterministic finite element simulations, experimental validation remains essential for capturing damage initiation and evolution mechanisms beyond the scope of numerical modeling. In this context, several non-destructive testing (NDT) techniques offer valuable pathways for future research. Active infrared thermography has been applied to composite materials as a non-contact method for detecting subsurface defects through abnormal thermal responses induced by external heating, providing advantages in inspection efficiency and operational safety compared to conventional techniques (Protasov, 2018). Ultrasonic-based approaches, such as ultrasonic pulse velocity measurements, have also been widely used to assess internal material integrity by correlating wave propagation characteristics with mechanical properties (Zarate et al., 2022). In addition, photoacoustic imaging, which combines optical excitation with acoustic signal detection, has shown promise in identifying surface cracks with enhanced spatial resolution using ultrasonic-range sensors (Akbar and Setiawan, 2016). The integration of such experimental diagnostics with FEM-based analysis would enable a more comprehensive assessment of composite performance, bridging numerical prediction with damage-sensitive validation.

Although impact behavior and damage progression are critical for certain structural appli-

cations, particularly those involving accidental or dynamic loading, their investigation is beyond the scope of this study. Future research may incorporate experimental techniques, such as impact testing, ultrasonic inspection, or thermographic methods, to evaluate damage initiation and propagation mechanisms, thereby complementing the finite element–based findings presented here.

4. Conclusions

The influence of fiber orientation and laminate configuration on the tensile and flexural behavior of sisal- and kenaf-fiber-reinforced epoxy composites was investigated using a finite element-based approach. The results demonstrate that the number of 0° plies plays a dominant role in determining load-bearing capacity, with a reduction in 0° laminates leading to a pronounced decrease in tensile strength, while ±45° plies showing a limited effect, and 90° plies consistently reducing axial performance. Kenaf-based composites exhibited higher elastic and flexural modulus, confirming their suitability for stiffness-dominated designs, whereas sisal-based composites provided superior tensile and flexural strength, making them more appropriate for strength-critical applications. Further, flexural analysis revealed that four-point bending produced higher stiffness values than three-point bending due to reduced shear influence. These findings highlight the effectiveness of laminate orientation as a mechanical tailoring tool for lightweight and renewable energy-supporting structures, where stiffness, weight, and deformation control are key design drivers. The limitation of this study is that the analysis is based on deterministic finite element simulations without experimental damage or fatigue characterization, which should be addressed in future work.

Acknowledgements

We sincerely thank Ahmad Rusdiansyah and Irma Noor Fitriastari for their invaluable assistance in proofreading this article. Their meticulous attention to detail and insightful feedback greatly enhanced the manuscript's clarity and quality.

Author Contributions

Londen Batan conceptualize the research and provided overall supervision. Pramono validated the mathematical equations. Alief Wikarta contributed to data supplementation. Suwarno evaluated the composition and structure of the article. Putu Suwarta evaluated the composite materials. Sze Wei Khoo reviewed and refined the numerical methods. Ubaidillah assisted in drafting and editing the manuscript. All authors have reviewed and approved the final version of the manuscript.

Conflict of Interest

The authors have no conflicts of interest to declare. No personal circumstances or interests have influenced the representation or interpretation of the results of this study.

References

Akbar, M., & Setiawan, R. (2016). Integrity assessment of cracked pressure vessel with considering effect of residual stress based on failure assessment diagram criteria. *Journal of Ocean, Mechanical and Aerospace -Science and Engineering-*, *28*, 16–24. https://doi.org/10.36842/jomase.v28i1.422

Alajmi, A., et al. (2022). An experimental and numerical investigation into the durability of fibre/polymer composites with synthetic and natural fibres. *Polymers*, *14*(10), 2024. https://www.mdpi.com/2073-4360/14/10/2024

Al-Ansari, L. S. (2014). Investigating the effect of volume fraction on the stress intensity factor for composite plate with central crack. https://www.researchgate.net/publication/282690308_Investigating_the_effect_of_volume_fraction_on_the_stress_intensity_factor_for_composite_plate_with_central_crack

Aravinth, K., Sathish, R., Ramakrishnan, T., Mahandiran, S. B., & Sundhar, S. S. (2023). Mechanical investigation of agave fiber reinforced composites based on fiber orientation, fiber length, and fiber volume fraction. *Materials Today: Proceedings*. https://linkinghub.elsevier.com/retrieve/pii/S2214785323030729

Ariyanti, M. Z., Tofrowaih, K. A., & Silvi. (2022). Effect of natural fibers reinforcement of honeycomb sandwich using numerical analysis. *International Journal of Technology*, *13*(4), 774–784. https://doi.org/10.14716/ijtech.v13i4.5098

Bharath, K. N. N., Roopa, D., Indran, S., Basavarajappa, S., Sanjay, M. R., & Siengchin, S. (2022). Influence of the stacking sequence and coconut husk micro fillers on the drilling parameters of coconut leaf sheath/glass/jute fiber hybrid phenol formaldehyde composites. *Materials Today: Proceedings*, *52*, 2427–2431. https://doi.org/10.1016/j.matpr.2021.10.422

Buragohain, M. K. (2017). *Composite structures: Design, mechanics, analysis, manufacturing, and testing*. CRC Press. https://www.taylorfrancis.com/books/mono/10.1201/9781315268057/composite-structures-manoj-kumar-buragohain

Cakiroglu, C., & Bekdas, G. (2021). Buckling analysis and stacking sequence optimization of symmetric laminated composite plates. In *Advances in structural engineering—optimization* (pp. 237–248). Springer. http://link.springer.com/10.1007/978-3-030-61848-3_9

Chandramohan, D., & Marimuthu. (2011). A review on natural fibers. *International Journal of Research and Reviews in Applied Sciences*, *8*(2), 194–206.

Cheung, H. Y., Ho, M. P., Lau, K. T., Cardona, F., & Hui, D. (2009). Natural fibre-reinforced composites for bioengineering and environmental engineering applications. *Composites Part B: Engineering*, *40*(7), 655–663. https://doi.org/10.1016/j.compositesb.2009.04.014

Chinta, V. S., Ravinder Reddy, P., & Eshwar Prasad, K. (2022). Experimental investigation of high cycle fatigue life of jute fibre reinforced hybrid composite material for axial flow fan blades. *Materials Today: Proceedings*, *59*, 357–367. https://doi.org/10.1016/j.matpr.2021.11.317

Chinta, V. S., Ravinder Reddy, P., & Prasad, K. E. (2022). The effect of stacking sequence on the tensile properties of jute fibre reinforced hybrid composite material for axial flow fan blades: An experimental and finite element investigation. *Materials Today: Proceedings*, *59*, 747–755. https://doi.org/10.1016/j.matpr.2021.12.500

Choudhury, A. K. R. (2014). Environmental impacts of the textile industry and its assessment through life cycle assessment. In *Roadmap to sustainable textiles and clothing* (pp. 1–39). Springer. https://doi.org/10.1007/978-981-287-110-7_1

Cutolo, A., Carotenuto, A. R., Palumbo, S., Esposito, L., Minutolo, V., Fraldi, M., & Ruocco, E. (2021). Stacking sequences in composite laminates through design optimization. *Meccanica*, *56*(6), 1555–1574. https://doi.org/10.1007/s11012-020-01233-y

Gebremichael, G., Mekonone, S. T., Baye, T. M., & Ejigu, A. A. (2025). Mechanical and microstructural characterization of sisal fiber-reinforced polyester laminate composites for improved durability in automotive applications. *Journal of Materials Science: Composites*, *6*(1), 1. https://doi.org/10.1186/s42252-024-00064-4

Giannitra, D. K., Kencanawati, C., & Negara, D. P. (2019). Karakteristik akustik dan mekanik dari green composite serat sabut kelapa (cocos nuciferal) bioresin getah pinus (pinus merkusii) dengan variasi waktu perlakuan alkali (naoh). *Proceedings*, 533–539.

Gupta, U. S., et al. (2021). Study on the effects of fiber orientation on the mechanical properties of natural fiber reinforced epoxy composite by finite element method. *Materials Today: Proceedings*, 7885–7893. https://doi.org/10.1016/j.matpr.2020.12.614

Islam, M. H., Islam, M. R., Dulal, M., Afroj, S., & Karim, N. (2022). The effect of surface treatments and graphene-based modifications on mechanical properties of natural jute fiber composites: A review. *iScience*, *25*(1), 103597. https://doi.org/10.1016/j.isci.2021.103597

Istana, B., Alfredo, F., & Sunaryo, S. (2024). Characterization of the mechanical properties of fiberglass/epoxy prepreg composites as horizontal axis wind turbine blade material: Influence of fiber orientation on impact and bending strength. *Jurnal Polimesin*, *22*(4), 457. https://doi.org/10.30811/jpl.v22i4.5363

Jaiswal, D., Devnani, G. L., Rajeshkumar, G., Sanjay, M. R., & Siengchin, S. (2022). Review on extraction, characterization, surface treatment and thermal degradation analysis of new cellulosic fibers as sustainable reinforcement in polymer composites. *Current Research in Green and Sustainable Chemistry*, *5*, 100271. https://doi.org/10.1016/j.crgsc.2022.100271

Jawaid, M., & Khalil, H. P. S. A. (2011). Cellulosic/synthetic fibre reinforced polymer hybrid composites: A review. *Carbohydrate Polymers*, *86*(1), 1–18. https://doi.org/10.1016/j.carbpol.2011.04.043

Joseph, K., Tolêdo Filho, R. D., James, B., Thomas, S., & Carvalho, L. H. (1999). A review on sisal fiber reinforced polymer composites. *Revista Brasileira de Engenharia Agrícola e Ambiental*, *3*(3), 367–379. https://doi.org/10.1590/1807-1929/agriambi.v3n3p367-379

Kalagi, G. R., Patil, R., & Nayak, N. (2018). Experimental study on mechanical properties of natural fiber reinforced polymer composite materials for wind turbine blades. *Materials Today: Proceedings*, 2588–2596. https://linkinghub.elsevier.com/retrieve/pii/S2214785317322757

Karthick, M., et al. (2022). Experimental investigation on mechanical properties of glass fiber hybridized natural fiber reinforced penta-layered hybrid polymer composite. *International Journal of Chemical Engineering*, *2022*, 1864446. https://doi.org/10.1155/2022/1864446

Kennedy, Z. E., & Inigo Raja M, A. (2022). Influence of stacking sequence and hybridization on the mechanical and tribological properties of glass and jute fiber composites. *Materials Today: Proceedings*, *55*, 220–225. https://doi.org/10.1016/j.matpr.2021.06.294

Kumpati, R., Skarka, W., Skarka, M., & Brojan, M. (2024). Enhanced optimization of composite laminates: Multi-objective genetic algorithms with improved ply-stacking sequences. *Materials*, *17*(4), 887. https://doi.org/10.3390/ma17040887

Malkapuram, R., Kumar, V., & Singh Negi, Y. (2009). Recent development in natural fiber reinforced polypropylene composites. *Journal of Reinforced Plastics and Composites*, *28*(10), 1169–1189. https://doi.org/10.1177/0731684407087759

Marin-Tellez, P., Lopez-Garza, V., Soriano-Pena, J. F., Marin-Tellez, G. J., & Santibanez-Maldonado, A. (2025). Structural evaluation of natural fiber composite materials for low-capacity wind turbine blades. *MRS Advances*, *10*(3), 316–321. https://doi.org/10.1557/s43580-024-01061-2

Miliket, T. A., Ageze, M. B., Tigabu, M. T., & Zeleke, M. A. (2022). Experimental characterizations of hybrid natural fiber-reinforced composite for wind turbine blades. *Heliyon*, *8*(3), e09092. https://doi.org/10.1016/j.heliyon.2022.e09092

Moraras, C. I., Goanta, V., Husaru, D., Istrate, B., Barsanescu, P. D., & Munteanu, C. (2023). Analysis of the effect of fiber orientation on mechanical and elastic characteristics at axial stresses of gfrp used in wind turbine blades. *Polymers*, *15*(4), 861. https://doi.org/10.3390/polym15040861

Naveen, J., Jawaid, M., Vasanthanathan, A., & Chandrasekar, M. (2019). Finite element analysis of natural fiber-reinforced polymer composites. In *Modelling of damage processes in biocomposites, fibre-reinforced composites and hybrid composites* (pp. 153–170). Elsevier. https://linkinghub.elsevier.com/retrieve/pii/B9780081022894000096

Owen, M. M., Wong, L. S., Achukwu, E. O., Romli, A. Z., Nazeri, M. N., & Shuib, S. (2024). Composites techniques optimization and finite element analysis of kenaf fiber reinforced

epoxy nonwoven composite structures for renewable energy infrastructure. *Journal of Industrial Textiles*, *54*, 15280837241283963. https://doi.org/10.1177/15280837241283963

Palani, S., Kumar R, R., D, R., K, R., J, M., & M, R. (2024). Mechanical characteristics of kenaf-glass fiber reinforced hybrid composites by varying the stacking sequences. *Physica Scripta*, *99*(10), 1059b3. https://doi.org/10.1088/1402-4896/ad79c7

Phunpeng, V., Boransan, W., & Horpibulsuk, S. (2023). Comprehensive analysis of in-plane tensile characteristics of hybrid composite using finite element method. *Journal of Engineering Research*. https://linkinghub.elsevier.com/retrieve/pii/S2307187723003139

Pickering, K. L., Efendy, M. G. A., & Le, T. M. (2016). A review of recent developments in natural fibre composites and their mechanical performance. *Composites Part A: Applied Science and Manufacturing*, *83*, 98–112. https://doi.org/10.1016/j.compositesa.2015.08.038

Polit, A. L., Soemardi, T. P., Purnama, H., & Olivier. (2021). Composite multiaxial mechanics: Laminate design optimization of taper-less wind turbine blades with ramie fiber-reinforced polylactic acid. *International Journal of Technology*, *12*(6), 1273–1287. https://doi.org/10.14716/ijtech.v12i6.5199

Prabaharan, T., Bejaxhin, A. B. H., Sankaran, S. K., Ramanan, N., & J, D. S. (2023). Comparative testing of tensile, flexural and impact analysis on coated and uncoated kenaf fiber reinforced composite. *Journal of Mines, Metals and Fuels*, 119–129. https://doi.org/10.18311/jmmf/2022/31211

Protasov, A. (2018). Active infrared testing of composites using 3d computer simulation. *International Journal of Technology*, *9*(3), 632. https://doi.org/10.14716/ijtech.v9i3.218

Purnowidodo, A., Anam, K., Darmadi, D. B., & Wahjudi, A. (2018). The effect of fiber orientation and stress ratio on the crack growth behaviour of fiber metal laminates (fmls). *International Journal of Technology*, *9*(5), 1039. https://doi.org/10.14716/ijtech.v9i5.853

Rahman, M. M., & Sultana, J. (2023). Design and optimization of natural fiber reinforced hybrid composite rve: A finite element analysis. *2023 International Conference on Engineering, Science and Advanced Technology (ICESAT)*, 204–209. https://ieeexplore.ieee.org/document/10347323/

Raj, E. F. I., et al. (2023). Natural-fibre-reinforced composite-based micro-size wind turbines: Numerical analysis and feasibility study. *Journal of Composites Science*, *7*(5), 197. https://www.mdpi.com/2504-477X/7/5/197

Rao, K. M. M., Rao, K. M., & Prasad, A. V. R. (2010). Fabrication and testing of natural fibre composites: Vakka, sisal, bamboo and banana. *Materials and Design*, *31*(1), 508–513. https://doi.org/10.1016/j.matdes.2009.06.023

Reddy, B. M., Reddy, R. M., Reddy, B. C. M., Reddy, P. V., Rao, H. R., & Reddy, Y. V. M. (2020). The effect of granite powder on mechanical, structural and water absorption characteristics of alkali treated cordia dichotoma fiber reinforced polyester composite. *Polymer Testing*, *91*, 106782. https://doi.org/10.1016/j.polymertesting.2020.106782

Reddy, P. V., Mohana Krishnudu, D., Rajendra Prasad, P., & R, V. S. R. (2021). A study on alkali treatment influence on prosopis juliflora fiber-reinforced epoxy composites. *Journal of Natural Fibers*, *18*(8), 1094–1106. https://doi.org/10.1080/15440478.2019.1687063

Samuel, B. O., Sumaila, M., & Dan-Asabe, B. (2024). Multi-objective optimization and modeling of a natural fiber hybrid reinforced composite for wind turbine blade development using grey relational analysis and regression analysis. *Mechanics of Advanced Materials and Structures*, *31*(3), 640–658. https://doi.org/10.1080/15376494.2022.2118404

Santhanam, V., & Chandrasekaran, M. (2014). Effect of surface treatment on the mechanical properties of banana-glass fibre hybrid composites. *Applied Mechanics and Materials*, *591*, 7–10. https://doi.org/10.4028/www.scientific.net/AMM.591.7

Saroj, S., & Nayak, R. K. (2021). Improvement of mechanical and wear resistance of natural fiber reinforced polymer composites through synthetic fiber hybridization. *Transactions*

of the Indian Institute of Metals, *74*(11), 2651–2658. https://doi.org/10.1007/s12666-021-02347-x

Selvan, E. V., Ponshanmugakumar, A., Ramanan, N., & Naveen, E. (2020). Determination and investigation of mechanical behaviour on kenaf-sisal hybrid composite. *Materials Today: Proceedings*, 3358–3362.

Sharba, M. J., Leman, Z., Sultan, M. T. H., Ishak, M. R., & Hanim, M. A. A. (2016). Tensile and compressive properties of woven kenaf/glass sandwich hybrid composites. *International Journal of Polymer Science*, *2016*, 1–6. https://doi.org/10.1155/2016/1235048

Shieddieque, A. D., Mardiyati, M., Suratman, R., & Widyanto, B. (2021). Preparation and characterization of sansevieria trifasciata fiber/high-impact polypropylene and sansevieria trifasciata fiber/vinyl ester biocomposites for automotive applications. *International Journal of Technology*, *12*(3), 549. https://doi.org/10.14716/ijtech.v12i3.2841

Sinitsky, O., Trabelsi, N., & Priel, E. (2022). The mechanical response of epoxy–sisal composites considering fiber anisotropy: A computational and experimental study. *Fibers*, *10*(5), 43. https://doi.org/10.3390/fib10050043

Sivakumar, D., Ng, L. F., Zalani, N. F. M., Selamat, M. Z., Ab Ghani, A. F., & Fadzullah, S. H. S. M. (2018). Influence of kenaf fabric on the tensile performance of environmentally sustainable fibre metal laminates. *Alexandria Engineering Journal*, *57*(4), 4003–4008. https://doi.org/10.1016/j.aej.2018.02.010

Sreenivas, H. T., Krishnamurthy, N., & Arpitha, G. R. (2020). A comprehensive review on lightweight kenaf fiber for automobiles. *International Journal of Lightweight Materials and Manufacture*, *3*(4), 328–337. https://doi.org/10.1016/j.ijlmm.2020.05.003

Sundar, D., Narasimalu, S., Yang, Y., & Sharma, S. (2017). Opportunities for natural fiber reinforced composites towards tropical wind turbine material needs. *Asian Conference on Energy, Power and Transportation Electrification (ACEPT)*, 1–7.

Supian, A. B. M., Asyraf, M. R. M., Syamsir, A., Ma, Q., Hazrati, K. Z., Azlin, M. N. M., Ali, M. M., Ghani, A., & Hua, L. S. (2024). Kenaf/glass fiber-reinforced polymer composites: Pioneering sustainable materials with enhanced mechanical and tribological properties. *Polymer Composites*, *45*(16), 14421–14447. https://doi.org/10.1002/pc.28785

Venkatesan, K., & Bhaskar, G. B. (2020). Evaluation and comparison of mechanical properties of natural fiber abaca-sisal composite. *Fibers and Polymers*, *21*(7), 1523–1534. https://doi.org/10.1007/s12221-020-9532-5

Wambua, P., Ivens, J., & Verpoest, I. (2003). Natural fibres: Can they replace glass in fibre reinforced plastics? *Composites Science and Technology*, *63*(9), 1259–1264. https://doi.org/10.1016/S0266-3538(03)00096-4

Wang, T., Song, B., Qiao, K., Ding, C., & Wang, L. (2019). Influence of the hybrid ratio and stacking sequence on mechanical and damping properties of hybrid composites. *Polymer Composites*, *40*(6), 2368–2380. https://doi.org/10.1002/pc.25096

Yusuff, I., Sarifuddin, N., & Ali, A. M. (2021). A review on kenaf fiber hybrid composites: Mechanical properties, potentials, and challenges in engineering applications. *Progress in Rubber, Plastics and Recycling Technology*, *37*(1), 66–83. https://doi.org/10.1177/1477760620953438

Zakaria, N. A., Ishak, M. R., Mustapha, F., & Yidris, N. (2023). Tensile properties of a hybrid kenaf-glass fibre composite shaft. *Materials Today: Proceedings*, *74*, 492–498. https://doi.org/10.1016/j.matpr.2022.12.016

Zarate, D. M., Cardenas, F., Forero, E. F., & Pena, F. O. (2022). Strength of concrete through ultrasonic pulse velocity and uniaxial compressive strength. *International Journal of Technology*, *13*(1), 103. https://doi.org/10.14716/ijtech.v13i1.4819